DOI: 10.1002/cphc.201402646

π-Expanded α,β-Unsaturated Ketones: Synthesis, Optical Properties, and Two-Photon-Induced Polymerization

Rashid Nazir,[a] Florent Bourquard,[b] Evaldas Balčiūnas,[b] Sabina Smoleń,[d] David Gray,[b] Nikolai V. Tkachenko,*[c] Maria Farsari,*[b] and Daniel T. Gryko*[a, d]

A library of π-expanded α,β-unsaturated ketones was designed and synthesized. They were prepared by a combination of Wittig reaction, Sonogashira reaction, and aldol condensation. It was further demonstrated that the double aldol condensation can be performed effectively for highly polarized styrene- and diphenylacetylene-derived aldehydes. The strategic placement of two dialkylamino groups at the periphery of D-π-A-π-D molecules resulted in dyes with excellent solubility. These ketones absorb light in the region 400–550 nm. Many of them display strong solvatochromism so that the emission ranges from 530–580 nm in toluene to the near-IR region in benzonitrile. Ketones based on cyclobutanone as central moieties display very high fluorescence quantum yields in nonpolar solvents, which decrease drastically in polar media. Photophysical studies of these new functional dyes revealed that they possess an enhanced two-photon absorption cross section when compared with simpler ketone derivatives. Due to strong polarization of the resulting dyes, values of two-photon absorption cross sections on the level of 200–300 GM at 800 nm were achieved, and thanks to that as well as the presence of the keto group, these new two-photon initiators display excellent performance so that the operating region is 5–75 mW in some cases.

1. Introduction

The increase in human life expectancy has increased demand for materials for tissue engineering and regenerative medicine. New biomaterials have been developed through object-oriented synthesis, blending, and modification that possess characteristics tailor-made for the applications they are aimed towards. One of the techniques used for the construction of biomedical implants and scaffolds for tissue engineering is direct laser writing (DLW) by two-photon-induced polymerization (TPIP). Since its first demonstration by Maruo in 1997, TPIP material engineering has developed to a level at which it is now possible to produce high-quality products of suitable design by computer-aided design.[1–6]

In TPIP, the tightly focused laser beam is used for the generation of radicals through the two-photon absorption (2PA) of a photoinitiator; these radicals induce the polymerization. The photopolymerization voxel is minimized by tightly focusing the laser beam using a high numerical aperture (NA) objective lens, and reducing the laser power and exposure time.[7,8]

Though a significant number of compounds possessing high 2PA cross sections (σ_2) have been developed, the majority of them have low solubility and/or a low yield of radical generation.[9–14] Consequently, the majority of TPIP research is still carried out using commercially available radical photoinitiators, usually with 2PA cross sections lower than 40 GM (GM = Goeppert–Mayer units), and hence they need large excitation powers and high exposure times.[15] In addition, many of these are compounds that are either toxic, or have components that could cause long-term damage to humans. Novel generations of photoinitiators tailored towards TPIP have been investigated over the last decade.[16–20] Herein, we present our research into photoinitiator molecules that at the same time possess large σ_2, strong TPIP photoinitiation potential, and excellent solubility in monomers, another key factor that is often overlooked.[16e]

We focused on ketones, since carbonyl groups are simultaneously one of the classic elements in photoinitiated polymerization[21] and also very strong electron acceptors. In addition, these molecules do not possess any moieties harmful to humans; they rather resemble the widely used natural food colorant turmeric. The aim of this study is to investigate systematically the effect of rigidity, size of π-conjugated systems,

---

[a] R. Nazir, Prof. Dr. D. T. Gryko
Warsaw University of Technology Faculty of Chemistry
Noakowskiego 3, 00-664 Warsaw (Poland)
E-mail: dtgryko@icho.edu.pl

[b] Dr. F. Bourquard, E. Balčiūnas, Dr. D. Gray, Dr. M. Farsari
Institute of Electronic Structure and Laser (IESL)
Foundation 50 for Research and Technology Hellas (FORTH)
711 10 Heraklion, Crete (Greece)
E-mail: mfarsari@iesl.forth.gr

[c] Prof. Dr. N. V. Tkachenko
Department of Chemistry and Bioengineering
Tampere University of Technology
33720 Tampere (Finland)
E-mail: nikolai.tkachenko@tut.fi

[d] Dr. S. Smoleń, Prof. Dr. D. T. Gryko
Institute of Organic Chemistry
Polish Academy of Sciences
Kasprzaka 44/52, Warsaw (Poland)

Supporting Information for this article is available on the WWW under http://dx.doi.org/10.1002/cphc.201402646.

and type of linker on the photoinitiating activity of quasi-quadrupolar α,β-unsaturated ketones.

2. Results and Discussion

Knowing that quadrupolar-like molecules possessing the same structural elements as dipolar molecules always have higher σ_2,[14] we focused our research on quadrupolar α,β-unsaturated ketones. To minimize conformational flexibility we selected only cycloalkanones as central units of these dyes.

Examples of bis(arylidene)cycloalkanones having the general formula D-π-A-π-D have already been reported and a number of them possess large σ_2.[22,23] Needless to say, the size of the middle ring has a major impact on the photochemical and photophysical properties of bis(arylidene)cycloalkanones.[17,24] The structural elements have been chosen in such a way to achieve high diversity and at the same time to allow us to cross-compare both optical properties and performance in TPIP of these compounds. Three different cyclic ketones, namely cyclobutanone (**8**), cyclopentanone (**9**), and 4-methylcyclohexanone (**10**), were selected as key building blocks, which allowed us to obtain dyes of different rigidity. As second building blocks we have chosen D-π-A-type aldehydes differing in the type of linker. Altogether six α,β-unsaturated ketones based on cycloalkanones were designed and synthesized.

4-(Didodecylamino)benzaldehyde was synthesized from aniline following a procedure described in the literature.[25] The dialkylamino styrene **4** was prepared through a Wittig-type approach starting from *N*,*N*-didodecylaniline (**1**).[25] The prepared phosphonium salt **2**[26] was subjected to Wittig condensation with terephthaldehyde diethyl acetal (**3**), followed by the removal of the acetal group under mild acidic conditions[27] (Scheme 1). Intermediate **5** (prepared in two steps from 4-iodoaniline[28]) was reacted with aldehyde **6** under Sila–Sonogashira reaction conditions[29] at room temperature to afford the desired push–pull aldehyde **7** (Scheme 2). All α,β-unsaturated ketones **11**–**16** were synthesized from 4-(didodecylamino)benzaldehyde or aldehydes **4** and **7** through classical aldol condensation using commercially available 4-*N*,*N*-dimethylaminobenzaldehyde or prepared aldehydes and the corresponding cycloketones (Table 1). Except for dye **16**, all double aldol condensations occurred smoothly and furnished final products at a yield of 69–99% as orange-red low-melting solids. All six dyes displayed excellent solubility in a majority of solvents.

Despite the strong structural similarity between ketones **11** and **12** (identical π system), the absorption spectra of these compounds are different (Figure 1, Table 2). The absorption maxima of **12**, the compound bearing long *n*-alkyl chains ($-C_{12}H_{25}$), are redshifted relative to **11** ($-CH_3$) both in toluene (587 cm^{-1}) and benzonitrile (611 cm^{-1}). On comparing compound **12** with **13**, it is well visible that π expansion of α,β-unsaturated ketones sometimes does not lead to an increase in their molar absorption coefficients (Figure 1). Higher absorptivity has been observed for dyes **14**–**16**, which possess different conformation being derivatives of more flexible cyclopentanone and 4-methylcyclohexanone (Figure 1). For compounds

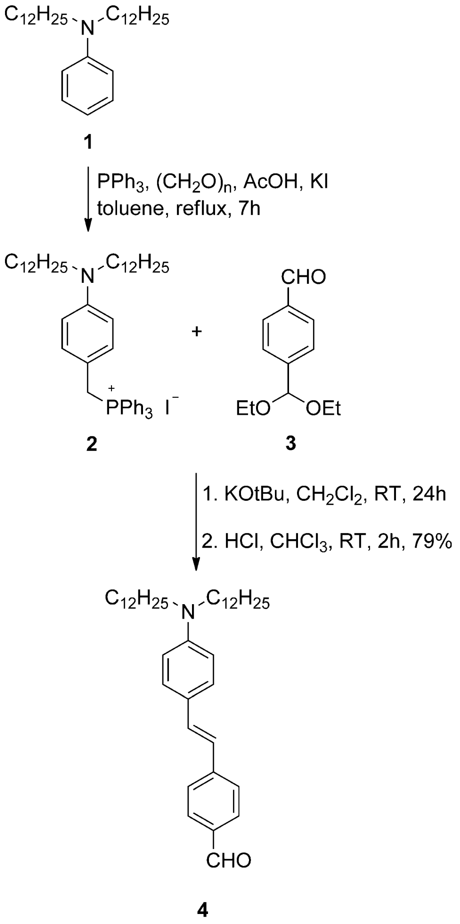

Scheme 1. Synthesis of (*E*)-4-[4-(didodecylamino)styryl]benzaldehyde.

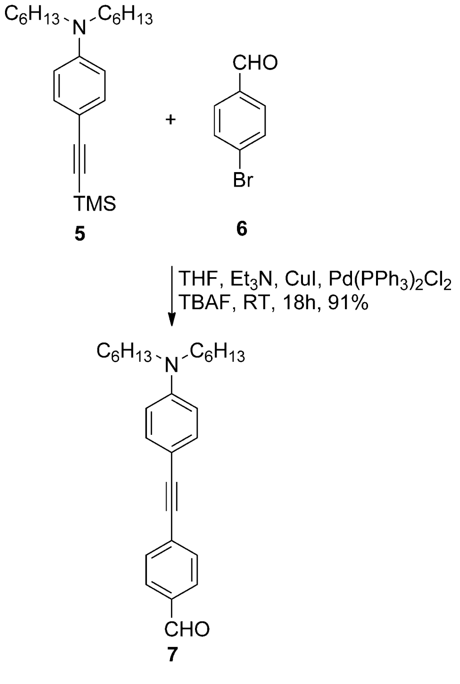

Scheme 2. Synthesis of 4-{[4-(dihexylamino)phenyl]ethynyl}benzaldehyde. TMS = trimethylsilyl, TBAF = tetrabutylammonium fluoride.

Table 1. Preparation of α,β-unsaturated ketones **11**–**16**.

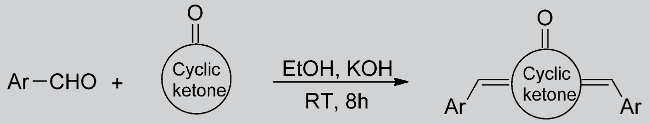

Aldehyde	Ar	Cyclic ketone		Unsaturated ketone	Yield [%]
	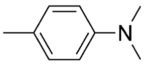	**8**	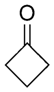	**11**	99
	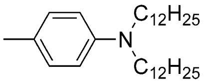	**8**	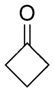	**12**	93
4	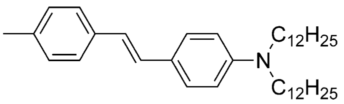	**8**	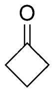	**13**	87
4	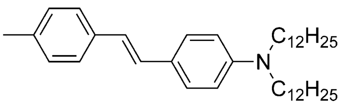	**9**	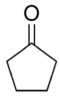	**14**	91
4	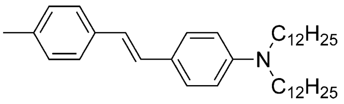	**10**	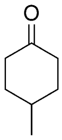	**15**	69
7	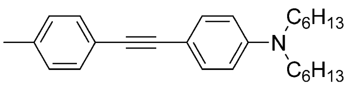	**9**	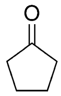	**16**	29

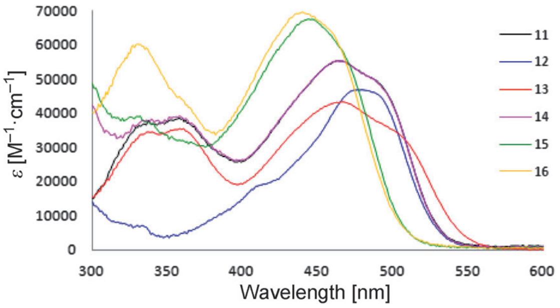

Figure 1. Absorption spectra of **11**–**16** in toluene.

Table 2. Photophysical properties of bis(arylidene)cycloalkanones **11**–**16** in toluene and benzonitrile.

Compound	Solvent	λ_{abs} [nm]	λ_{em} [nm]	$\Delta\nu$ [cm^{-1}]	Φ_{fl}
11	toluene	476	530	2100	0.16
	benzonitrile	488	591	3600	0.36
12	toluene	477	533	2200	0.19
	benzonitrile	503	591	3100	0.29
13	toluene	467	583	4300	0.74
	benzonitrile	488	705	6300	< 0.01
14	toluene	466	556	3500	0.72
	benzonitrile	487	764	7400	< 0.01
15	toluene	444	540	4000	0.40
	benzonitrile	460	742	8300	< 0.01
16	toluene	440	536	4100	0.14
	benzonitrile	458	793	9200	< 0.01

13–**15**, which possess extended π systems (styryl–benzylidene), one can observe a correlation between the size of the alicyclic middle ring and the position of the absorption band (Figure 1, Table 2). Absorption maxima of **15** (cyclohexanone ring) are significantly blueshifted (≈1100 cm^{-1}) relative to **13** (cyclobutanone ring) and **14** (cyclopentanone ring) both in toluene and benzonitrile. These results are in agreement with the literature.[24] On comparing compounds **14** and **16**, which possess the same alicyclic ring (cyclopentanone), one can observe a blueshift of absorption maximum for **16**, the dye bearing two C≡C triple bonds. This is in full agreement with the work presented by Meier,[30] who pointed out that C=C double bonds are more polarizable than C≡C triple bonds (which result in a decrease in the HOMO–LUMO gap). Furthermore, all newly synthesized dyes **11**–**16** exhibit positive solvatochromism, thus suggesting a larger polarization in the excited state than in the ground state.

There is no significant difference in the emission spectra of **11** and **12** (Figure 2, Table 2). For all compounds the Stokes shift is larger in benzonitrile than in toluene, in agreement with the assumption that these newly synthesized dyes exhibit a greater dipole moment in the excited state than in the ground state. A change in dipole moment requires solvent re-

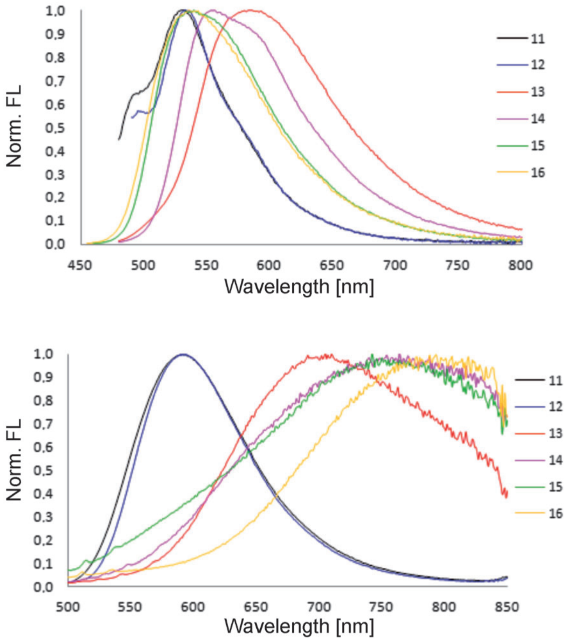

Figure 2. Normalized emission spectra of **11**–**16** in: a) toluene, b) benzonitrile.

Table 3. Fluorescence emission lifetimes obtained by TCSPC for **11**–**16** ($\lambda_{ex}=483$ nm).

Compound	Solvent	τ_1 [ns]	Relative amplitude	τ_2 [ns]	Relative amplitude	τ_3 [ns]	Relative amplitude	$\chi^{2[a]}$
11	toluene	0.29	0.97	0.82	0.03	–	–	1.07
	benzonitrile	1.34	0.72	0.22	0.28	–	–	1.10
12	toluene	0.34	0.83	0.68	0.17			1.17
	benzonitrile	1.27	0.82	0.35	0.18	–	–	1.18
13	toluene	1.93	1	–	–			1.09
	benzonitrile	0.06	51	0.58	35	1.38	14	1.04
14	toluene	1.35	1	–	–			1.05
	benzonitrile	0.19	0.91	1.40	0.09	–	–	1.09
15	toluene	0.68	0.73	0.96	0.27			1.09
	benzonitrile	0.16	0.99	1.92	0.01	–	–	1.23
16	toluene	0.33	0.72	1.03	0.28			0.83
	benzonitrile	0.25	0.99	1.10	0.01	–	–	1.00

[a] Data fit weighted mean square deviation.

organization, which makes the Stokes shift sensitive to the solvent polarity. The Stokes shift depends on the reorganization energy and the reorganization energy is greater in solvents with greater dielectric constant. The emission maxima of compounds **13**–**15** are blueshifted, as are their absorption spectra. With an increase in the size of the middle ring, for **13**–**15**, compounds possessing the same π system, one can observe a decrease in fluorescence quantum yield (Φ_{fl}). A larger ring provides greater movement flexibility, thus promoting nonradiative relaxation of electronically excited states. A significant redshift of the emission maxima in benzonitrile in **13**–**16** may be due to the formation of excited charge-transfer states. Furthermore, their fluorescence quantum yields decrease significantly when the solvent polarity increases, and do not exceed 1% (Table 1), thus indicating that for **13**–**16** in benzonitrile the charge separation is almost complete. The latter also explains an interesting phenomenon observed on comparing the optical properties of ketones **11** and **12** with π-expanded ketones **13**–**16**. On moving from **11** and **12** to **13**–**16** one can observe a small bathochromic shift of absorption;[30] at the same time there is a strong bathochromic shift of emission depending strongly on the solvent.

The fluorescence lifetimes for **11**–**16** were obtained after biexponential fitting of the emission decays, though in most cases there is one dominating component. The lifetimes are given in Table 3, together with the relative amplitudes of each decay component with the first being the dominating one. In the case of **11** and **12**, the fluorescence lifetimes in benzonitrile are appreciably longer than in toluene. One reason for this might be the significant difference in viscosity between benzonitrile and toluene, which can result in limiting the nonradiative decay mechanism.

The fluorescence lifetimes of **13**–**16** vary in a similar manner to the fluorescence quantum yields: the lifetime shortens with an increase in size of the alicyclic ring. For **13**–**16** in benzonitrile, a short-lived component, $\tau=190$–250 ps, was observed, which indicates faster nonradiative decay of the excited state compared to that of **11** and **12** in qualitative agreement with the fluorescence quantum yields presented in Table 2.

For compounds **11**–**16**, the transient absorption spectra were measured with the pump–probe technique in toluene and benzonitrile. In the case of **11** and **12** in both solvents, decomposition of samples by laser beam was observed. For other compounds reasonably good agreement between emission decays and transient absorption measurements was observed. Fluorescence decay measurements for **13** in toluene give a 1.93 ns lifetime for the singlet state; therefore, the transient absorption spectrum component with time constant of 2.2 ns can definitely be attributed to the decay of the singlet state (Figure S1 a in the Supporting Information). The triplet-state spectrum (after 2.2 ns decay) is very weak. For **14** in toluene the singlet state decays with a time constant of 100 ps and the long-lived state (after 100 ps decay) is the triplet state (Figure S1 b). Similarly to **14**, the longest-lived state for **15** is the triplet excited state, and the spectrum at 550 ps is the spectrum of the thermally equilibrated excited singlet state (Figure S1 c). In the case of **16**, the spectrum of the triplet state has much lower relative intensity than that for **14** and **15**. Otherwise its behavior is similar to that of the previously mentioned compounds. Like before, the lifetimes of the singlet state obtained from transient absorption and fluorescence

Table 4. Comparison of excited singlet-state lifetimes obtained by pump–probe system ($\tau_{p\text{-}p}$) and fluorescence emission (τ_{em}) measurements.

Compound	Solvent	Singlet $\tau_{p\text{-}p}$ [ps]	Singlet τ_{em} [ps]	Triplet/singlet[a]
13	toluene	2200 ± 340	1930	≈ 0.1
		(320 ± 75)		
	benzonitrile	730 ± 220	1110	0
		(100 ± 25)	190	
14	toluene	880 ± 60	1350	0.3
	benzonitrile	150 ± 15	190	0
15	toluene	550 ± 30	680	0.5
16	toluene	310 ± 30	330	0.15
	benzonitrile	195 ± 12	250	0

[a] Triplet/singlet is calculated as the ratio of the maximum of triplet-state differential absorption in the red–near-IR part of the spectrum to that of the singlet after fast (< 50 ps) relaxation.

emission measurements agree well with each other, in this case, 310 and 330 ps, respectively (Figure S1 d, Table 4).

The spectra of **13**–**16** in benzonitrile vary considerably from those measured in toluene. For all samples there is no detectable trace of triplet state formed after singlet-state relaxation. In the case of **14**, the singlet excited state decays with a time constant of 150 ps, which is in good agreement with fluorescence lifetime measurements of 190 ps (Figure S2 b). For **15** in benzonitrile, the negative absorbance in the 750–1000 nm range is definitely due to the stimulated emission, since there is no ground-state absorption in this range (Figure S2 c). Therefore the process with 130 ps time constant is a decay of the singlet excited state. The emission decay time constant obtained from time-correlated single photon counting (TCSPC) measurements is 160 ps, which also agrees well with the 130 ps time constant and its interpretation as the singlet excited-state lifetime (Table 4). No indication of triplet state is observed for **16** in benzonitrile (Figure S2 d). The singlet-state lifetimes obtained from fluorescence and absorption decay measurements are in reasonably good agreement at 250 and 200 ps, respectively (Table 4).

2.1. Two-Photon Absorption

Two-photon absorption cross sections were measured through the *Z*-scan technique at 800 nm (Table 5). The values are generally in the range 50–370 GM, that is, significantly higher than in the case of 4,4′-bis(diethylamino)benzophenone (**R**), though one has to remember that the maximum of the 2PA can be located at different values from 800 nm for two reasons. First of all, dyes **11**–**16** differ in the size of their π-conjugated system. Secondly, although all studied molecules are symmetrical (C_2) they are not centrosymmetrical. Consequently g→c and g→e transitions should both be observable in the 2PA spectrum.[31] As a result, two-photon spectra of these dyes have to possess two bands, and the band that could be ascribed to the S_0–S_1 transition is most probably more intense than the higher-energy S_0–S_2 transition.[31]

Table 5. 2PA cross section values of the compounds **11**–**16** measured by *Z*-scan at 800 nm.

Compound	Solvent	Concentration [mol L⁻¹]	σ_2 [GM]
11	CH_3Cl_3	0.05	70
12	CH_2Cl_2	0.01	140
13	CH_2Cl_2	0.01	50
14	CH_2Cl_2	0.01	130
15	CH_2Cl_2	0.01	200
16	CH_2Cl_2	0.01	370
R	1-propanol	0.25	7

The highest σ_2 value (at 800 nm) has been measured for dye **16**, which possesses cyclopentanone as a central unit and a C≡C bond as linker.

2.2. Fabrication Properties

The one-photon potential of the synthesized photoinitiators was investigated by polymerizing drop-cast films of the material under a wide-spectrum UV lamp. The fabrication window (FW) is the power difference between the polymerization threshold and the burning threshold. Having a large FW is beneficial, as it allows the use of higher powers and indicates the possibility of using the material at industrial scales.

The threshold value, damage threshold, and FW of the synthesized compounds are presented in Figure 3. As reference, we used 4,4′-bis(diethylamino)benzophenone, a commercially available photoinitiator used widely in TPIP.

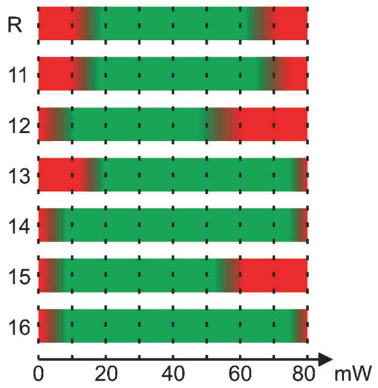

Figure 3. 2PA FW values of the compounds **11**–**16** and **R** (4,4′-bis(diethylamino)benzophenone). The low-power end shows polymerization thresholds (red and green interface), whereas the burning threshold is represented in the high-power end of the scale.

Compounds **11**–**16** (1 %, w/w) were added to the hybrid material and the photopolymerization thresholds were determined by polymerizing structures at different laser powers. The upper limit of the polymerization window corresponds to material being burned. The overall performance in TPIP can be evaluated by two factors: 1) the increase of 2PA cross section; and 2) photofragmentation of ketones, which is the key step since it affects the production of radicals. It is clearly visible that compounds **14** and **16** possess the broadest FW (Figure 3). π Expansion improves the polymerization threshold from about 15 mW to approximately 5 mW (**14**–**16** versus **11**).

For the derivative of 4-methylcyclohexanone **15**, the burning threshold is the lowest, which may originate from the lower yield of photofragmentation into radicals.

To explore the effectiveness of the synthesized TPIP photoinitiators, 2D and 3D grid structures (Figure 4) were fabricated by DLW using different laser powers. Figure 4A shows a 3D structure obtained by using a laser power in the middle of the FW; it can be seen that it is built accurately and has a well-defined topography. Figure 4B presents a structure built by using a laser power near the polymerization threshold. As the material had not polymerized fully, the structure could not survive the development process and collapsed. Figure 4C shows 3D structures under different laser powers. The laser power increases from the left to the right. Figure 4D and 4E show 2D structures built using powers in the middle of the FW and at the polymerization threshold, respectively. Again, the structure fabricated at the polymerization threshold is distorted due to incomplete polymerization. Figure 4F presents 2D structures under different laser powers increasing from the left to the right.

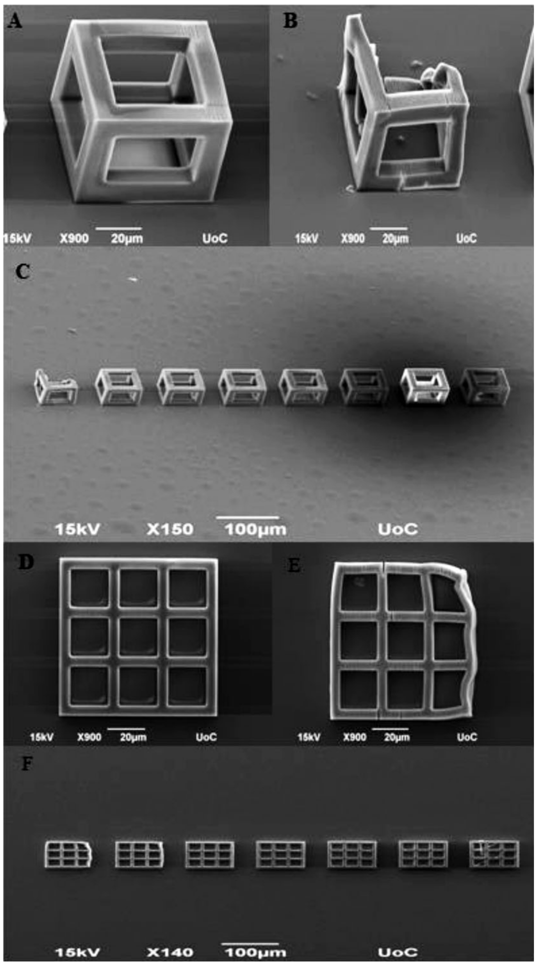

Figure 4. Typical microstructures fabricated under three different conditions using compound **16** as initiator: A) good structuring 3D, B) polymerization threshold 3D, C) 3D structures under different laser power, D) good structuring 2D, E) polymerization threshold 2D, F) 2D structures under different laser power. UoC = University of Crete

3. Conclusions

A synthetic route to novel two-photon photoinitiators has been presented. We have demonstrated that π-expanded α,β-unsaturated ketones with D-π-A-π-D structure possess large intrinsic 2PA in the near-IR range of wavelengths, with maximum values of $\sigma_2 \approx 370$ GM. The introduction of peripheral dialkylamino groups proved to be an excellent strategy to achieve at the same time strong charge-transfer character and good solubility of π-expanded ketones. As a result, a very broad FW has been achieved in DLW (5–75 mW), which compares favorably with that of previous TPIP initiators. The other notable findings are as follows: 1) the π expansion of quadrupolar α,β-unsaturated ketones typically leads to only small changes in both molar absorption coefficients and position of the absorption maxima (Figure 1); 2) the fluorescence quantum yield of these solvatochromic dyes depends strongly on the polarity of the solvent; and 3) the ketone possessing the highest 2PA cross section is the best overall performer, which emphasizes the critical influence of the 2PA cross section.

Experimental Section

Materials and Synthesis

All commercially available compounds were used as purchased. The reaction progress was monitored by thin-layer chromatography (TLC) with silica gel 60 F254 (Merck) with detection by UV lamp. *N*,*N*-Didodecylaniline[25] (**1**), 4-(didodecylamino)benzaldehyde,[25] *N*,*N*-dihexyl-4-iodoaniline,[32] and *N*,*N*-dihexyl-4-[(trimethylsilyl)ethynyl]aniline (**5**)[33] were obtained by the reported methods.

N,*N*-Didodecyl-4-[(iodotriphenylphosphoranyl)methyl]aniline (**2**): A mixture of *N*,*N*-didodecylaniline (4.71 g, 11 mmol), triphenylphosphine (2.88 g, 11 mmol), paraformaldehyde (0.33 g, 3.7 mmol), potassium iodide (1.65 g, 11 mmol), water (0.75 mL), and acetic acid (2.22 mL) in toluene (30 mL) was heated at reflux for 7 h. After addition of water (40 mL), the resulting mixture was extracted with CH_2Cl_2, and the combined organic layers were washed with aq $NaHCO_3$ and water and dried over Na_2SO_4. The solvent was evaporated, and the residue was recrystallized with methanol and used as such for the next step. HRMS (ESI): *m*/*z*: calcd for $C_{49}H_{72}NP$: 704.5324 $[M+H]^+$; found: 704.5326.

(*E*)-4-[4-(Didodecylamino)styryl]benzaldehyde (**4**): Compound **2** (1.40 g, 2 mmol), terephthalaldehyde mono(diethylacetal) (**3**, 0.499 g, 2.40 mmol), and *t*BuOK (0.268 g, 2.40 mmol) were mixed in dry CH_2Cl_2 (20 mL) at 0 °C under argon. The resulting mixture was stirred at room temperature for 24 h, then the solvent was removed under reduced pressure and the crude acetal was hydrolyzed using 10% HCl (25 mL) in $CHCl_3$ (50 mL) at 25 °C for 1 h. The two layers were separated and the organic layer was washed with aq $NaHCO_3$, dried over Na_2SO_4, and evaporated to dryness. The residue was dissolved in CH_2Cl_2, a catalytic amount of iodine was added, and this solution was stirred at 25 °C for 3 h under illumination (75 W lamp). The resulting mixture was washed with aq $Na_2S_2O_3$ and dried over Na_2SO_4. After evaporation of the solvent, the crude product was purified by dry column vacuum chromatography (DCVC;[34] silica, hexanes/CH_2Cl_2 1:1) to give **4** in the form of a yellow solid with 79% yield. Physical properties corresponded with the published data.[35]

4-{[4-(Dihexylamino)phenyl]ethynyl}benzaldehyde (**7**): A stirred solution of **6** (370 mg, 2.0 mmol), **5** (714 mg, 2.0 mmol), $PdCl_2(PPh_3)_2$ (100 mg, 0.1 mmol), and CuI (20 mg, 0.1 mmol) in triethylamine (10 mL) and tetrahydrofuran (10 mL) was flushed with argon for 15 min at room temperature. Then tetrabutylammonium fluoride (2.5 mL, 1 M in THF, 2.5 mmol) was added dropwise and the resulting solution was stirred overnight at room temperature. Subsequently, the reaction mixture was extracted with ethyl acetate and water (50 mL each), and the combined organic layers were washed with water and brine and dried over Na_2SO_4. Purification by DCVC (silica, dichloromethane/hexanes 1:2 to 1:1) gave the desired compound **7** as an orange oil (719 mg, 92 %). Physical properties corresponded with the published data.[28]

General Procedure for Synthesis of α,β-Unsaturated Ketones 11–16

A mixture of aromatic aldehyde (1 mmol), cyclic ketone (0.5 mmol), and KOH (56 mg, 1 mmol) in ethanol (5 mL) was stirred at 40 °C for 8 h (the reaction progress was monitored by TLC analysis). Then, solvent was removed and the crude product was purified by recrystallization or by column chromatography.

(2*E*,4*E*)-2,4-Bis[4-(dimethylamino)benzylidene]cyclobutanone (**11**): Yield 99 %. The product was purified by crystallization from absolute ethanol to afford **11** as red crystals. ^1H NMR (500 MHz, $CDCl_3$): $\delta = 7.48$ (d, $J = 9$ Hz, 4 H), 7.14 (s, 2 H), 6.72 (d, $J = 8.5$ Hz, 4 H), 3.73 (s, 2 H), 3.04 ppm (s, 12 H); ^{13}C NMR (125 MHz, $CDCl_3$) $\delta = 190.7$, 151.3, 141.3, 131.6, 127.1, 123.2, 112.1, 40.3, 35.2 ppm; HRMS (ESI): *m/z*: calcd for $C_{22}H_{25}N_2O$: 332.1889 $[M+H]^+$; found: 332.1894.

(2*E*,4*E*)-2,4-Bis[4-(didodecylamino)benzylidene]cyclobutanone (**12**): Yield 93 %. Purification by DCVC (silica, CH_2Cl_2/hexanes 1:1) provided the product as a red gel. ^1H NMR (500 MHz, $CDCl_3$): $\delta = 7.45$ (d, $J = 8.5$ Hz, 4 H), 7.12 (s, 2 H), 6.63 (d, $J = 8.5$ Hz, 4 H), 3.72 (s, 2 H), 3.32 (t, $J = 14.5$ Hz, 8 H), 1.61–160 (m, 8 H), 1.32–1.26 (m, 72 H), 0.89 ppm (t, $J = 14$ Hz, 12 H); ^{13}C NMR (125 MHz, $CDCl_3$) $\delta = 190.7$, 149.3, 141.1 131.8, 129.7, 124.3, 111.6, 51.2, 45.1, 35.2, 32.0, 29.79, 29.75, 29.6, 29.4, 27.4, 27.2, 26.9, 22.8, 14.2 ppm; HRMS (ESI): *m/z*: calcd for $C_{66}H_{112}N_2ONa$: 971.8679 $[M+Na]^+$; found: 971.8672.

(2*E*,4*E*)-2,4-Bis{4-[(*E*)-4-(didodecylamino)styryl]benzylidene}cyclobutanone (**13**): Yield 87 %. Purification by DCVC (silica, CH_2Cl_2/hexanes 2:1) afforded the product as a red gel. ^1H NMR (500 MHz, $CDCl_3$): $\delta = 7.55$–7.50 (m, 8 H), 7.41 (d, $J = 9$ Hz, 4 H), 7.23 (d, $J = 4.5$ Hz, 2 H), 7.14 (d, $J = 16.5$ Hz, 2 H), 6.90 (d, $J = 17$ Hz, 2 H), 6.63 (d, $J = 9$ Hz, 4 H), 3.88 (s, 2 H), 3.30 (t, $J = 15$ Hz, 8 H), 1.59–1.56 (m, 8 H), 1.32–1.27 (m, 72 H), 0.90 ppm (t, $J = 13.5$ Hz, 12 H); ^{13}C NMR (125 MHz, $CDCl_3$) $\delta = 189.8$, 148.0, 138.8, 136.9, 134.6, 134.1, 131.0, 130.1, 128.0, 125.7, 124.1, 122.7, 111.5, 51.0, 36.7, 31.9, 29.67, 29.64, 29.62, 29.54, 29.36, 27.3, 27.1, 22.7, 21.7, 14.1 ppm; HRMS (ESI): *m/z*: calcd for $C_{82}H_{125}N_2O$: 1153.9792 $[M+H]^+$; found: 1153.9788.

(2*E*,5*E*)-2,5-Bis{4-[(*E*)-4-(didodecylamino)styryl]benzylidene}cyclopentanone (**14**): Purification by DCVC (silica, CH_2Cl_2/hexanes 2:1) afforded the product as a red gel with 91 % yield. ^1H NMR (500 MHz, $CDCl_3$): $\delta = 7.59$–7.51 (m, 10 H), 7.40 (d, $J = 9$, 4 H), 7.10 (d, $J = 16.5$ Hz, 2 H), 6.90 (d, $J = 16$ Hz, 2 H), 6.63 (d, $J = 9.5$ Hz, 4 H), 3.30 (t, $J = 15$ Hz, 8 H), 3.15 (s, 4 H), 1.59–1.53 (m, 8 H), 1.32–1.27 (m, 72 H), 0.901 ppm (t, $J = 14$ Hz, 12 H); ^{13}C NMR (125 MHz, $CDCl_3$) $\delta = 196.3$, 148.2, 139.7, 136.8, 134.2, 133.6, 131.4, 130.6, 128.2, 126.3, 124.2,122.7, 111.7, 51.2, 32.0, 29.8, 29.78, 29.76, 29.6, 29.57, 29.50, 27.4, 27.3, 26.8, 22.8, 14.2 ppm; HRMS (ESI): *m/z*: calcd for $C_{83}H_{127}N_2O$: 1167.9948 $[M+H]^+$; found: 1167.9935.

(2*E*,6*E*)-2,6-Bis{4-[(*E*)-4-(didodecylamino)styryl]benzylidene}-4-methylcyclohexanone (**15**): Yield 69 %. Purification by DCVC (silica, CH_2Cl_2/hexanes 2:1) afforded the product as a red gel. ^1H NMR (500 MHz, $CDCl_3$): $\delta = 7.78$ (s, 2 H), 7.50–7.37 (m, 12 H), 7.11 (d, $J = 16$ Hz, 2 H) 6.89 (d, $J = 16$ Hz, 2 H), 6.62 (d, $J = 9$ Hz, 4 H), 3.29 (t, $J = 15$ Hz, 8 H), 3.12–3.09 (m, 2 H) 2.57–2.52 (m, 2 H), 1.91–1.89 (m, 1 H), 1.60 (m, 8 H), 1.32–1.22 (m, 72 H), 1.11 (d, $J = 6.5$ Hz, 3 H), 0.89 ppm (t, $J = 14$ Hz, 12 H); ^{13}C NMR (125 MHz, $CDCl_3$) $\delta = 190.0$, 148.1, 139.0, 137.0, 134.8, 134.2, 131.1, 130.2, 128.1, 125.9, 124.2, 122.9, 111.7, 51.1, 36.8, 32.0, 29.8, 29.76, 29.75, 29.67, 29.49, 29.3, 27.45, 27.30, 22.8, 21.8, 14.2 ppm; HRMS (ESI): *m/z*: calcd for $C_{85}H_{131}N_2O$: 1196.0261 $[M+H]^+$; found: 1196.0255.

(2*E*,5*E*)-2,5-Bis(4-{[4-(dihexylamino)phenyl]ethynyl}benzylidene)cyclopentanone (**16**): Purification by DCVC (silica, CH_2Cl_2/hexanes 2:1) afforded the product as a red gel with 29 % yield. ^1H NMR (500 MHz, $CDCl_3$): $\delta = 7.57$–7.52 (m, 10 H), 7.38 (d, $J = 9$ Hz, 4 H), 6.58 (d, $J = 9.5$ Hz, 4 H), 3.29 (t, $J = 15$ Hz, 8 H), 3.14 (s, 4 H), 1.60–1.57 (m, 8 H), 1.33–1.32 (m, 24 H), 0.92 ppm (t, $J = 13.5$ Hz, 12 H); ^{13}C NMR (125 MHz, $CDCl_3$) $\delta = 196.1$, 148.3, 137.5, 134.7, 133.4, 133.1, 131.5, 130.7, 125.6, 111.3, 108.4, 93.9, 87.5, 51.1, 31.9, 27.3, 26.9, 26.7, 22.8, 14.1 ppm; HRMS (ESI): *m/z*: calcd for $C_{59}H_{75}N_2O$: 827.5879 $[M+H]^+$; found: 827.5886.

Resin Preparation

The resin used in this work was an organic–inorganic zirconium silicate described in detail earlier.[12] For these experiments, it was prepared as described previously.[19]

Photophysics

All photophysical studies were conducted at room temperature in spectrometric-grade solvents: toluene with dielectric constant $\varepsilon = 2.38$ (23 °C) and benzonitrile with $\varepsilon = 25.9$ (20 °C).[36] Steady-state absorption spectra of **11**–**16** were recorded in a 1 cm quartz cuvette by using a Shimadzu UV-3600 spectrophotometer in the 300–800 nm wavelength region. Absorption and fluorescence measurements for compounds **11**–**16** were performed at a dye concentration of 0.01–0.05 mol L^{-1} depending on the dye. Steady-state emission spectra were recorded using a Horiba Jobin Yvon Fluorolog-3-111 fluorescence spectrophotometer. The samples were excited at the first absorption maximum. The fluorescence quantum yields of **11**–**16** were calculated using fluorescein ($\Phi_f = 0.79$ in ethanol) as a standard.[37] For each sample, refractive index corrections were taken into account. Fluorescence lifetimes in the nanosecond timescale were determined by using a time-correlated single photon counting (TCSPC) method (PicoQuant GmbH, including the PicoHarp 300 controller, LDH-P-C-485 diode laser, and PDL 800-B driver). Samples were excited near the absorption maximum (483 nm) and monitored at the emission maximum. The excitation repetition rate was 10 MHz and a typical time resolution was 150 ps. The transient absorption spectra for **11**–**16** were measured with a pump–probe system, with a time resolution of approximately 100 fs. The pump wavelength was 420 nm. Absorption was monitored in both 470–760 and 840–1060 nm wavelength ranges.

Z-Scan Technique

The experimental setup to measure 2PA cross sections using the *Z*-scan technique was described earlier;[19b] however, the laser pulse duration used was shorter (60 fs instead of 250 fs; see the Supporting Information for details). *Z*-scan measurements for compounds **11**–**16** and **R** were performed at a dye concentration of 0.01–0.25 mol$\,$L^{-1} depending on the dye.

Fabrication of Microstructures

The experimental setup and procedure for the fabrication of 3D structures by TPIP has been described previously.[38] In this case, a Ti:sapphire femtosecond laser (Femtolasers Fusion, 800 nm, 75 MHz, <20 fs) was focused tightly into the volume of the photosensitive hybrid material by using a high-NA microscope objective lens (100×, NA $=1.4$, Zeiss, Plan Apochromat). The average laser power was measured before the objective, and the scanning velocity was 2 mm$\,$s^{-1}. After the completion of the fabrication process, the samples were developed for 20 min in 4-methyl-2-pentanone.

Acknowledgements

The research leading to these results has received funding from the European Community's Seventh Framework Marie Curie ITN programs TopBio (PITN-GA-2010-264362) and AngioMatTrain (PITN-GA-2012- 317304).

Keywords: aldol reaction · ketones · photosensitizers · polymerization · two-photon absorption

[1] S. Maruo, O. Nakamura, S. Kawata, *Opt. Lett.* **1997**, *22*, 132 – 134.

[2] A. Radke, T. Gissibl, T. Klotzbucher, P. V. Braun, H. Giessen, *Adv. Mater.* **2011**, *23*, 3018 – 3021.

[3] N. Vasilantonakis, K. Terzaki, I. Sakellari, V. Purlys, D. Gray, C. M. Soukoulis, M. Vamvakaki, M. Kafesaki, M. Farsari, *Adv. Mater.* **2012**, *24*, 1101 – 1105.

[4] Y.-S. Chen, A. Tal, S. M. Kuebler, *Chem. Mater.* **2007**, *19*, 3858 – 3860.

[5] J. K. Gansel, M. Thiel, M. S. Rill, M. Decker, K. Bade, V. Saile, G. von Freymann, S. Linden, M. Wegener, *Science* **2009**, *325*, 1513 – 1515.

[6] M. T. Raimondi, S. M. Eaton, M. Lagana, V. Aprile, M. M. Nava, G. Cerullo, R. Osellame, *Acta Biomater.* **2013**, *9*, 4579 – 4584.

[7] a) K. S. Lee, D. Y. Yang, S. H. Park, R. H. Kim, *Polym. Adv. Technol.* **2006**, *17*, 72 – 82; b) A. I. Ciuciu, P. Cywiński, *RSC Adv.* **2014**, *4*, 45504 – 45516; c) A. Selimis, V. Mironov, M. Farsari, *Microelectron. Eng.* **2015**, *132*, 83 – 89.

[8] H. B. Sun, K. Takada, M. S. Kim, K. S. Lee, S. Kawata, *Appl. Phys. Lett.* **2003**, *83*, 1104 – 1106.

[9] M. A. Albota, D. Beljonne, J. L. Bredas, J. E. Ehrlich, J. Y. Fu, A. A. Heikal, S. E. Hess, T. Kogej, M. D. Levin, S. R. Marder, D. McCord-Maughon, J. W. Perry, M. Rumi, G. Subramaniam, W. W. Webb, S. L. Wu, C. Xu, *Science* **1998**, *281*, 1653 – 1656.

[10] S. J. Chung, K. S. Kim, T. C. Lin, G. S. He, J. Swiatkiewicz, P. N. Prasad, *J. Phys. Chem. B* **1999**, *103*, 10741 – 10745.

[11] K. D. Belfield, A. R. Morales, J. M. Hales, D. J. Hagan, E. W. Van Stryland, V. M. Chapela, J. Percino, *Chem. Mater.* **2004**, *16*, 2267 – 2273.

[12] A. Ovsianikov, J. Viertl, B. Chichkov, M. Oubaha, B. MacCraith, I. Sakellari, A. Giakoumaki, D. Gray, M. Vamvakaki, M. Farsari, C. Fotakis, *ACS Nano* **2008**, *2*, 2257 – 2262.

[13] a) G. S. He, L.-S. Tan, Q. Zheng, P. N. Prasad, *Chem. Rev.* **2008**, *108*, 1245 – 1330; b) H. M. Kim, B. R. Cho, *Acc. Chem. Res.* **2009**, *42*, 863 – 872; c) M. Tasior, V. Hugues, M. Blanchard-Desce, D. T. Gryko, *Asian J. Org. Chem.* **2013**, *2*, 669 – 673; d) D. Firmansyah, A. I. Ciuciu, V. Hugues, M. Blanchard-Desce, L. Flamigni, D. T. Gryko, *Chem. Asian J.* **2013**, *8*, 1279 – 1294.

[14] a) M. Pawlicki, H. A. Collins, R. G. Denning, H. L. Anderson, *Angew. Chem. Int. Ed.* **2009**, *48*, 3244 – 3266; *Angew. Chem.* **2009**, *121*, 3292 – 3316; b) H. M. Kim, B. R. Cho, *Chem. Commun.* **2009**, 153 – 164; c) F. Terenziani, C. Katan, E. Badaeva, S. Tretiak, M. Blanchard-Desce, *Adv. Mater.* **2008**, *20*, 4641 – 4678.

[15] K. J. Schafer, J. M. Hales, M. Balu, K. D. Belfield, E. W. Van Stryland, D. J. Hagan, *J. Photochem. Photobiol. A* **2004**, *162*, 497 – 502.

[16] a) F. Hao, Z. Liu, M. Zhang, J. Liu, S. Zhang, J. Wu, H. Zhou, Y. P. Tian, *Spectrochim. Acta Part A* **2014**, *118*, 538 – 542; b) G. von Freymann, A. Ledermann, M. Thiel, I. Staude, S. Essig, K. Busch, M. Wegener, *Adv. Funct. Mater.* **2010**, *20*, 1038 – 1052; c) N. Pucher, A. Rosspeintner, V. Satzinger, V. Schmidt, G. Gescheidt, J. Stampfl, R. Liska, *Macromolecules* **2009**, *42*, 6519 – 6528; d) W. E. Lu, X. Z. Dong, W. Q. Chen, Z. S. Zhao, X.-M. Duan, *J. Mater. Chem.* **2011**, *21*, 5650 – 5659; e) C. N. LaFratta, J. T. Fourkas, T. Baldacchini, R. A. Farrer, *Angew. Chem. Int. Ed.* **2007**, *46*, 6238 – 6258; *Angew. Chem.* **2007**, *119*, 6352 – 6374.

[17] Z. Q. Li, N. Pucher, K. Cicha, J. Torgensen, S. C. Ligon, A. Ajami, W. Husinsky, A. Rosspeintner, E. Vauthey, S. Naumov, T. Scherzer, J. Stampfl, R. Liska, *Macromolecules* **2013**, *46*, 352 – 361.

[18] a) I. Fitilis, M. Fakis, I. Polyzos, V. Giannetas, P. Persephonis, *J. Photochem. Photobiol. A* **2010**, *215*, 25 – 30; <lit b>J.-F. Xing, W.-Q. Chen, X.-Z. Dong, T. Tanaka, X.-Y. Fang, X.-M. Duan, S. Kawata, *J. Photochem. Photobiol. A* **2007**, *189*, 398 – 404; c) K. S. Lee, R. H. Kim, D.-Y. Yang, S. H. Park, *Prog. Polym. Sci.* **2008**, *33*, 631 – 681; d) J. Gu, W. Yulan, W. Q. Chen, X. Z. Dong, X.-M. Duan, S. Kawata, *New J. Chem.* **2007**, *31*, 63 – 68; e) J. F. Xing, W.-Q. Chen, J. Gu, X.-Z. Dong, N. Takeyasu, T. Tanaka, X.-M. Duan, S. Kawata, *J. Mater. Chem.* **2007**, *17*, 1433 – 1438; f) T. Griesser, A. Wolfberger, U. Daschiel, V. Schmidt, A. Fian, A. Jerrar, C. Teichert, W. Kern, *Polym. Chem.* **2013**, *4*, 1708 – 1714; g) J. Xing, J. Liu, T. Zhang, L. Zhang, M. Zheng, X.-M. Duan, *J. Mater. Chem. B* **2014**, *2*, 4318 – 4323; h) I. Polyzos, G. Tsigaridas, M. Fakis, V. Giannetas, P. Persephonis, J. Mikroyannidis, *Chem. Phys. Lett.* **2003**, *369*, 264 – 268.

[19] a) R. Nazir, P. Danilevicius, A. I. Ciuciu, M. Chatzinikolaidou, D. Gray, L. Flamigni, M. Farsari, D. T. Gryko, *Chem. Mater.* **2014**, *26*, 3175 – 3184; b) R. Nazir, P. Danilevicius, D. Gray, M. Farsari, D. T. Gryko, *Macromolecules* **2013**, *46*, 7239 – 7244.

[20] a) M. Jin, H. Hong, J. Xie, J.-P. Malval, A. Spangenberg, O. Soppera, D. Wan, H. Pu, D.-L. Versace, T. Leclerc, P. Baldeck, O. Poizat, S. Knopf, *Polym. Chem.* **2014**, *5*, 4747 – 4755; b) A. Spangenberg, J.-P. Malval, H. Akdas-Kilig, J.-F. Fillaut, F. Stehlin, N. Hobeika, F. Morlet-Savary, O. Soppera, *Macromolecules* **2012**, *45*, 1262 – 1269.

[21] a) M. A. Tehfe, F. Dumur, B. Graff, D. Gigmes, J. P. Fouassier, J. Lalevée, *Macromolecules* **2013**, *46*, 3332 – 3341; b) M. A. Tehfe, F. Dumur, B. Graff, D. Gigmes, F. Morlet-Savary, J. P. Fouassier, D. Gigmes, J. Lalevéem, *Macromolecules* **2013**, *46*, 3761 – 3770; c) P. Xiao, F. Dumur, T. T. Bui, F. Goubard, B. Graff, F. Morlet-Savary, J. P. Fouassier, D. Gigmes, J. Lalevée, *ACS Macro. Lett.* **2013**, *2*, 736 – 740; d) P. Xiao, F. Dumur, D. Thirion, S. Fagour, A. Vacher, X. Sallenave, F. Morlet-Savary, B. Graff, J. P. Fouassier, D. Gigmes, J. Lalevée, *Macromolecules* **2013**, *46*, 6786 – 6793; e) P. Xiao, F. Dumur, B. Graff, D. Gigmes, J. P. Fouassier, J. Lalevée, *Macromolecules* **2013**, *46*, 7661 – 7667.

[22] E. A. Badaeva, T. V. Timofeeva, A. Masunov, S. Tretiak, *J. Phys. Chem. A* **2005**, *109*, 7276 – 7284.

[23] J. Xue, Y. Zhao, F. Wu, D.-C. Fang, *J. Phys. Chem. A* **2010**, *114*, 5171 – 5179.

[24] Q. Zou, Y. Zhao, N. S. Makarov, J. Campo, H. Yuan, D. C. Fang, J. W. Perry, F. Wu, *Phys. Chem. Chem. Phys.* **2012**, *14*, 11743 – 11752.

[25] T. Ozturk, A. S. Klymchenko, A. Capan, S. Oncul, S. Cikrikci, S. Taskiran, B. Tasan, F. B. Kaynak, S. Ozbey, A. P. Demchenko, *Tetrahedron* **2007**, *63*, 10290 – 10299.

[26] L. Porres, B. K. G. Bhatthula, M. Blanchard-Desce, *Synthesis* **2003**, 1541 – 1544.

[27] O. Mongin, L. Porres, M. Charlot, C. Katan, M. Blanchard-Desce, *Chem. Eur. J.* **2007**, *13*, 1481 – 1498.

[28] O. Mongin, L. Porres, L. Moreaux, J. Mertz, M. Blanchard-Desce, *Org. Lett.* **2002**, *4*, 719 – 722.

[29] Z. L. Zhou, L. Zhao, S. Zhang, K. Vincent, S. Lam, D. Henze, *Synth. Commun.* **2012**, *42*, 1622 – 1631.

[30] H. Meier, *Angew. Chem. Int. Ed.* **2005**, *44*, 2482 – 2506; *Angew. Chem.* **2005**, *117*, 2536 – 2561.

[31] a) G. Lemercier, C. Martineau, J.-C. Mulatier, I. Wang, O. Stéphan, P. Baldeck, C. Andraud, *New J. Chem.* **2006**, *30*, 1606 – 1613; b) G. Ponterini, D. Vanossi, Z. A. Krasnaya, A. S. Tatikolov, F. Momicchioli, *Phys. Chem. Chem. Phys.* **2014**, *16*, 15576 – 15589; c) K. M. Shafeekh, S. Das, C. Sissa, A. Painelli, *J. Phys. Chem. B* **2013**, *117*, 8536 – 8546.

[32] F. Diederich, F. Mitzel, P. Seller, C. Boudon, J.-P. Gisselbrecht, M. Gross, *Helv. Chim. Acta* **2004**, *87*, 1130 – 1157.
[33] C. Rouxel, M. Charlot, O. Mongin, T. R. Krishna, A. M. Caminade, J. P. Majoral, M. Blanchard-Desce, *Chem. Eur. J.* **2012**, *18*, 16450 – 16462.
[34] D. S. Pedersen, C. Rosenbohm, *Synthesis* **2001**, 2431 – 2434.
[35] S. Yagai, Y. Nakano, S. Seki, A. Asano, T. Okubo, T. Isoshima, T. Karatsu, A. Kitamura, Y. Kikkawa, *Angew. Chem. Int. Ed.* **2010**, *49*, 9990 – 9994; *Angew. Chem.* **2010**, *122*, 10186 – 10190.
[36] D. R. Lide, *Handbook of Organic Solvents*, CRC Press, Boca Raton, **1995**.
[37] R. E. Kellogg, R. G. Bennett, *J. Chem. Phys.* **1964**, *41*, 3042 – 3045.
[38] I. Sakellari, E. Kabouraki, D. Gray, V. Purlys, C. Fotakis, A. Pikulin, N. Bityurin, M. Vamvakaki, M. Farsari, *ACS Nano* **2012**, *6*, 2302 – 2311.

Received: September 18, 2014
Revised: November 17, 2014

R. Nazir, F. Bourquard, E. Balčiūnas, S. Smoleń, D. Gray, N. V. Tkachenko, M. Farsari,* D. T. Gryko**

■■ – ■■

π-Expanded α,β-Unsaturated Ketones: Synthesis, Optical Properties, and Two-Photon-Induced Polymerization

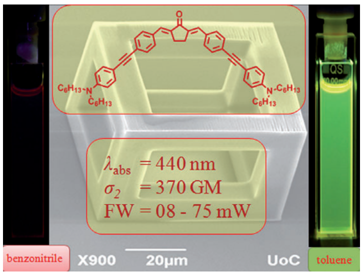

Expansion benefits: Photoinitiators for two-photon-induced polymerization, which comprise π-expanded α,β-unsaturated ketones with D-π-A-π-D structure, possess large intrinsic two-photon absorption cross sections (σ_2) in the near-IR range, strong solvatochromism, good solubility, and a broad fabrication window (FW; see figure).